11th AIAA/CEAS Aeroacoustics Conference, 23-25 May 2005, Monterey, CA, USA

Modal Scattering at an Impedance Transition in a Lined Flow Duct

Sjoerd W. Rienstra*

Eindhoven University of Technology, 5600 MB Eindhoven, The Netherlands.

Nigel Peake†

University of Cambridge, Cambridge CB3 0WA, UK.

An explicit Wiener-Hopf solution is derived to describe the scattering of duct modes at a hard-soft wall impedance transition in a circular duct with uniform mean flow. Specifically, we have a circular duct $r = 1, -\infty < x < \infty$ with mean flow Mach number $M > 0$ and a hard wall along $x < 0$ and a wall of impedance Z along $x > 0$. A minimum edge condition at $x = 0$ requires a continuous wall streamline $r = 1 + h(x,t)$, no more singular than $h = \mathcal{O}(x^{1/2})$ for $x \downarrow 0$.

A mode, incident from $x < 0$, scatters at $x = 0$ into a series of reflected modes and a series of transmitted modes. Of particular interest is the role of a possible instability along the lined wall in combination with the edge singularity. If one of the "upstream" running modes is to be interpreted as a downstream-running instability, we have an extra degree of freedom in the Wiener-Hopf analysis that can be resolved by application of some form of Kutta condition at $x = 0$, for example a more stringent edge condition where $h = \mathcal{O}(x^{3/2})$ at the downstream side. The question of the instability requires an investigation of the modes in the complex frequency plane and therefore depends on the chosen impedance model, since $Z = Z(\omega)$ is essentially frequency dependent.

The usual causality condition by Briggs and Bers appears to be not applicable here because it requires a temporal growth rate bounded for all real axial wave numbers. The alternative Crighton-Leppington criterion, however, is applicable and confirms that the suspected mode is usually unstable.

In general, the effect of this Kutta condition is significant, but it is particularly large for the plane wave at low frequencies and should therefore be easily measurable. For $\omega \to 0$, the modulus tends to $|R_{001}| \to (1+M)/(1-M)$ without and to 1 with Kutta condition, while the end correction tends to ∞ without and to a finite value with Kutta condition. This is exactly the same behaviour as found for reflection at a pipe exit with flow, irrespective if this is uniform or jet flow.

Nomenclature

E	=	entire function, viz. a constant
J_m	=	ordinary Bessel function of the first kinds of order m
h	=	perturbed position wall streamline
m	=	circumferential modal wave number
M	=	Mach number
μ, ν	=	radial modal order
$\boldsymbol{n}$	=	unit outer normal vectors at $r = 1$
$\boldsymbol{v}, p, \rho, c, \phi$	=	time-harmonic velocity, pressure, density, sound speed, potential perturbations
x, r, θ, t	=	axial, radial, azimuthal angle, time coordinate
$\boldsymbol{e}_x, \boldsymbol{e}_r, \boldsymbol{e}_\theta$	=	unit vectors in x, r, θ-direction
$\alpha_{m\nu}$	=	radial modal wave number
γ	=	reduced radial wave number

*Associate Professor, Department of Mathematics & Computer Science, Eindhoven University of Technology, P.O. Box 513, 5600 MB Eindhoven, The Netherlands. AIAA Member.

†Professor, Department of Applied Mathematics & Theoretical Physics, University of Cambridge, Centre for Mathematical Sciences, Wilberforce Road, Cambridge CB3 0WA, United Kingdom. AIAA member.

κ	=	axial wave number
σ	=	reduced axial wave number
$\sigma_{m\nu}$,	=	reduced axial modal wave number hard-wall duct
$\tau_{m\nu}$,	=	axial modal wave number soft-wall duct
ψ	=	scattered potential
ω	=	angular frequency; Helmholtz number
Ω	=	reduced frequency

I. Introduction

SOUND transmission through a lined flow duct may be described by a sum of modes if geometry, lining and mean flow are independent of the axial coordinate. Mathematically, modes (in some cases including a continuous spectrum) form a complete basis for the representation of the sound field, but physically, they are each also (self-similar) solutions of the equations. Therefore, they provide much insight into the physical behaviour of the sound propagation. Most of our knowledge of duct acoustics is based on understanding the modes.

The modes in lined circular ducts with uniform mean flow are nearly completely understood.[1] With hard walls we have a finite number of cut-on (axially propagating) and infinitely many cut-off (axially exponentially decaying) modes. With soft walls this difference is slightly blurred; all modes decay exponentially but some are weakly cut-off while the others are heavily cut-off. Apart from this difference in axial direction, there is also a marked difference in the cross-wise (radial) direction. Most modes are present throughout the duct, but some exist only near the wall. They decay exponentially in the radial direction away from the wall. These modes are called surface waves. Some exist both with and without flow, but some only with mean flow (of either type at most 2 per circumferential order for a hollow duct, 4 for an annular duct). The ones that exist only with mean flow are thus called hydrodynamic surface waves.[1]

By analogy with the Helmholtz instability along an interface between two media of different velocities, it was recognised by Ffowcs Williams and Tester[2] that one such hydrodynamic surface wave may have the character of an instability. This means that the mode seems to propagate in the upstream direction while it decays exponentially, but in reality its direction of propagation is downstream and it increases exponentially. Tester[2] verified this conjecture by the causality argument of Briggs and Bers[3–5] (using physically reasonable frequency dependent impedance models) and found that the suspected surface wave indeed may be an instability, at least according to the Briggs-Bers formalism. This was confirmed analytically by Rienstra in [1] for an incompressible limit of waves along an impedance of mass-spring-damper type, but now using the related causality criterion of Cright & Leppington.[12,26]

Extending these ideas, Koch and Möhring[6] analysed by a generalised Wiener-Hopf solution the scattered sound field in a 2D duct with mean flow and a *finite* lined section. Their (Briggs-Bers) causality analysis was slightly incomplete because they considered only frequency independent impedances, but otherwise they found results similar to Tester. If there is no instability wave available, the liner's leading edge singularity could be no less than rather strong. If there is an instability this singularity can be weak, similar to the Kutta condition for a trailing edge[a]. The singularity at the liner's trailing edge is more difficult to model[9,10] (the proper modelling may well be a nonlinear one and involve essentially a finite thickness mean flow boundary layer) and the scattering by this edge may add a certain amount of uncertainty to the results. This, however, is greatly overshadowed by the fact that the field obtained in the lined section becomes exponentially large when the instability is included. This is in the greatest contrast with any experimental evidence, apart from some weak indication reported by Ffowcs Williams.[11]

It is therefore still an open question if these modes are really unstable, or maybe essentially nonlinear for any reasonable acoustic amplitude because of the very high amplification rate.

On the other hand, this is not very unlike the situation for the jet. In agreement with theory, an instability indeed emerges from the exit edge, but further downstream the predicted Helmholtz instability is much less than is observed, because it quickly reaches the nonlinear regime. Still the major predicted acoustic consequences due to the excitation of the instability are very well described by linear theory[12–25] and it makes sense to investigate a common situation.

In the jet exit problem we know that the instability may be excited by vortex shedding from a sharp edge. In the inviscid models we are dealing with, the vortex shedding is enforced by application of the Kutta condition.[7,23] By analogy we propose here the canonical problem of a duct, consisting of a semi-infinite hard-walled section and a semi-infinite lined section, with a mean flow that runs from the hard-walled to the soft-walled parts. The liner instability,

[a] This Kutta condition essentially results from a delicate balance between viscous effects, nonlinear inertia and acceleration, described by a form of triple deck theory.[7,8] It would be of interest to investigate if any consistent high-Reynolds triple deck or otherwise structure is possible that is compatible with an absent instability and no Kutta condition.

if available, will be excited by application of some form of Kutta condition. Rather than the Briggs-Bers criterion (BB) we will use the Crighton-Leppington[12,26] causality test (CL), because, as we will show, BB is not applicable here, while it gives sometimes different answers than CL. In the cases considered, the suspected mode is more often detected as an instability by CL than by BB.

Similar problems were proposed for the semi-infinite 2D problems[27,28] and for the 2D duct with a finite lined section.[6] Unfortunately, in all these cases the acoustically detectable difference between the situation with and without an instability is relatively small and experimental verification seems difficult. We will show that in the low Helmholtz number limit of a circular duct there results a very large acoustical difference between presence and absence of the instability. In similar problems for the exhaust jet it has been shown experimentally that the excitation of an instability is really physical and the effect on the acoustics is just as big as the theory predicts.[16,18–21]

Although the present problem might be solved for most practical engineering purposes in a satisfactory way by mode matching, this method is not useful here as it provides no control of the edge singularity other than a posteriori by checking the convergence rate of the modal amplitudes. A much better approach in this respect is the Wiener-Hopf technique.[29] The problem of sound scattered in a semi-infinite duct is very apt to be treated by this method, while the edge singularity plays a most prominent role via the order of a polynomial function.

The pioneering Wiener-Hopf solution by Heins & Feshbach[30] without flow is almost as classical as the related problem for the unflanged pipe exit by Levine & Schwinger,[31] but we will not follow their approach. To include flow and Kutta condition in a convenient way, we will use a 3D version of the 2D analysis outlined in [28].

II. The problem

We assume a $e^{i\omega t}$-sign convention, while the exponent is dropped throughout. Consider the problem of the scattering of duct modes at a hard-soft wall impedance transition in a circular duct of radius a with uniform mean flow velocity U_0, density ρ_0 and soundspeed c_0 (see figure 1). Following[1] we make dimensionless: lengths on a, time on a/c_0, velocities on c_0, densities on ρ_0, and pressures on $\rho_0 c_0^2$. Noting that in uniform flow pressure, vorticity and entropy perturbations are decoupled, we leave vorticity and entropy perturbations unspecified and consider only the pressure field.

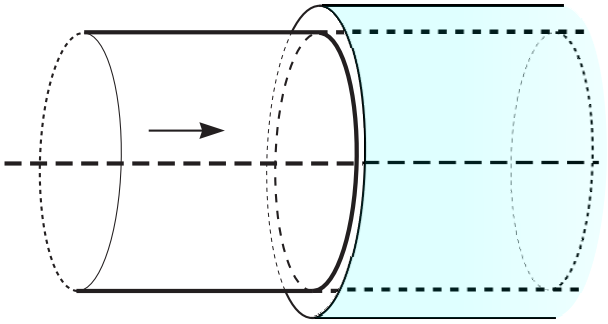

Figure 1. Sketch of geometry.

In particular, we have in a circular duct $r = 1, -\infty < x < \infty$ with uniform mean flow Mach number $M = U_0/c_0 > 0$ and a hard wall along $x < 0$ and a wall of impedance Z along $x > 0$ the time-harmonic acoustic field, with frequency $\omega > 0$, that satisfies

$$\left(i\omega + M\frac{\partial}{\partial x}\right)^2 p - \nabla^2 p = 0, \tag{1a}$$

$$\left(i\omega + M\frac{\partial}{\partial x}\right)\boldsymbol{v} + \nabla p = 0, \tag{1b}$$

with Ingard-Myers boundary conditions[32,33] along $r = 1$

$$x < 0: \qquad (\boldsymbol{v} \cdot \boldsymbol{e}_r) = 0, \tag{2a}$$

$$x > 0: \quad i\omega Z(\boldsymbol{v} \cdot \boldsymbol{e}_r) = \left(i\omega + M\frac{\partial}{\partial x}\right)p, \tag{2b}$$

while the field is regular at $r = 0$. Note that $Z = Z(\omega)$ in some physically suitable way. Assume the incident (i.e. rightrunning) mode in the hard-walled part $x < 0$

$$p_{\text{in}} = \mathrm{J}_m(\alpha_{m\mu} r)\, \mathrm{e}^{-\mathrm{i}m\theta - \mathrm{i}\kappa_{m\mu} x} \tag{3}$$

where $m \geq 0$, J_m is the m-th order ordinary Besselfunction of the first kind[34]. $-\alpha_{m\mu}^2$ is an eigenvalue of the Laplace operator in a circular cross section with Neumann boundary conditions, and given by

$$\alpha_{m\mu}^{1-m}\, \mathrm{J}'_m(\alpha_{m\mu}) = 0, \tag{4}$$

i.e. the non-trivial zeros of J'_m. $\alpha_{m\mu}$ is usually called the radial modal wave number. The axial modal wave number $\kappa_{m\mu}$ is defined through the dispersion relation

$$\alpha_{m\mu}^2 + \kappa_{m\mu}^2 = (\omega - M\kappa_{m\mu})^2 \tag{5}$$

such that the branch is taken with $\mathrm{Re}(\kappa_{m\mu}) > 0$ if the mode is cut-on or $\mathrm{Im}(\kappa_{m\mu}) < 0$ if the mode is cut-off. Due to circumferential symmetry, the scattered wave will depend on θ via $\mathrm{e}^{-\mathrm{i}m\theta}$ only, and we will from here on assume that $p := p\, \mathrm{e}^{-\mathrm{i}m\theta}$ where the exponent will be dropped.

After introducing the velocity potential with $\boldsymbol{v} = \nabla\phi$, we can integrate (1b) to get

$$\Big(\mathrm{i}\omega + M\frac{\partial}{\partial x}\Big)\phi + p = 0. \tag{6}$$

(The integration constant is not important.) So we have for the corresponding incident mode

$$\phi_{\text{in}} = \frac{\mathrm{i}}{\omega - M\kappa_{m\mu}} p_{\text{in}}. \tag{7}$$

We introduce the scattered part ψ of the potential by

$$\phi = \phi_{\text{in}} + \psi. \tag{8}$$

It is convenient to reformulate the boundary condition by way of the wall stream line given by

$$r = 1 + \mathrm{Re}\big(h(x)\, \mathrm{e}^{\mathrm{i}\omega t - \mathrm{i}m\theta}\big). \tag{9}$$

We have then at $r = 1$ (note that $\frac{\partial}{\partial r}\phi_{\text{in}} = 0$ at $r = 1$)

$$\frac{\partial\psi}{\partial r} = 0 \qquad \text{for } x < 0, \tag{10a}$$

$$\frac{\partial\psi}{\partial r} = \Big(\mathrm{i}\omega + M\frac{\partial}{\partial x}\Big)h \quad \text{for } x > 0, \tag{10b}$$

$$p = \mathrm{i}\omega Z h \qquad \text{for } x > 0. \tag{10c}$$

We expect some singular behaviour at $x = 0$, but no more than what goes together with a continuous wall streamline, so $h(0) = 0$ and $h(x+) \leq \mathcal{O}(x^\eta)$ for a $\eta > 0$.

III. The Wiener-Hopf analysis

We introduce the Fourier transforms to x

$$\hat{\psi}(\kappa, r) = \int_{-\infty}^{\infty} \psi(x, r)\, \mathrm{e}^{\mathrm{i}\kappa x}\, \mathrm{d}x, \tag{11a}$$

$$H_+(\kappa) = \int_0^{\infty} h(x)\, \mathrm{e}^{\mathrm{i}\kappa x}\, \mathrm{d}x, \tag{11b}$$

$$P_-(\kappa) = \int_{-\infty}^{0} \Big(\mathrm{i}\omega + M\frac{\partial}{\partial x}\Big)\psi(x, 1)\, \mathrm{e}^{\mathrm{i}\kappa x}\, \mathrm{d}x, \tag{11c}$$

to obtain for $\hat{\psi}$ the Bessel-type equation

$$\frac{\partial^2\hat{\psi}}{\partial r^2}+\frac{1}{r}\frac{\partial\hat{\psi}}{\partial r}+\left[(\omega-M\kappa)^2-\kappa^2-\frac{m^2}{r^2}\right]\hat{\psi}=0. \tag{12}$$

We introduce the reduced frequency Ω, Fourier wavenumber σ and radial wave number γ as follows.

$$\begin{gathered}\beta=\sqrt{1-M^2},\quad \omega=\beta\Omega,\quad \kappa=\frac{\Omega}{\beta}(\sigma-M)\\ \Omega\gamma=\sqrt{(\omega-M\kappa)^2-\kappa^2}=\Omega\sqrt{1-\sigma^2},\quad \gamma=\sqrt{1-\sigma^2}\quad \text{where}\ \ \mathrm{Im}(\gamma)\le 0.\end{gathered} \tag{13}$$

With (10a), (10b) and (11b) we arrive at the solution

$$\hat{\psi}=A(\sigma)\,\mathrm{J}_m(\Omega\gamma r), \tag{14a}$$

$$A(\sigma)=\mathrm{i}\frac{1-M\sigma}{\beta\gamma\,\mathrm{J}'_m(\Omega\gamma)}H_+. \tag{14b}$$

Since

$$\Big(\mathrm{i}\omega+M\frac{\partial}{\partial x}\Big)\psi=p_{\mathrm{in}}-p, \tag{15}$$

we have along the wall $r=1$

$$\mathrm{i}(\omega-M\kappa)A\,\mathrm{J}_m(\Omega\gamma)=P_-+\int_0^\infty p_{\mathrm{in}}\,\mathrm{e}^{\mathrm{i}\kappa x}\,\mathrm{d}x-\int_0^\infty p\,\mathrm{e}^{\mathrm{i}\kappa x}\,\mathrm{d}x, \tag{16}$$

which reduces to

$$\mathrm{i}(\omega-M\kappa)A\,\mathrm{J}_m(\Omega\gamma)=P_-+\frac{\mathrm{i}\,\mathrm{J}_m(\alpha_{m\mu})}{\kappa-\kappa_{m\mu}}-\mathrm{i}\omega Z H_+, \tag{17}$$

and

$$-\frac{\Omega}{\beta^2}(1-M\sigma)^2\frac{\mathrm{J}_m(\Omega\gamma)}{\gamma\,\mathrm{J}'_m(\Omega\gamma)}H_+ +\mathrm{i}\beta\Omega Z H_+=P_-+\frac{\mathrm{i}\beta\,\mathrm{J}_m(\alpha_{m\mu})}{\Omega(\sigma-\sigma_{m\mu})} \tag{18}$$

where we introduced

$$\sigma_{m\mu}=\sqrt{1-\frac{\alpha_{m\mu}^2}{\Omega^2}}, \tag{19}$$

such that $\mathrm{Re}(\sigma_{m\mu})>0$ and $\mathrm{Im}(\sigma_{m\mu})=0$, or $\mathrm{Im}(\sigma_{m\mu})<0$. This yields

$$P_-(\sigma)+\frac{\mathrm{i}\beta\,\mathrm{J}_m(\alpha_{m\mu})}{\Omega(\sigma-\sigma_{m\mu})}=-K(\sigma)H_+(\sigma), \tag{20}$$

where the Wiener-Hopf kernel K is defined by

$$K(\sigma)=\frac{\Omega}{\beta^2}(1-M\sigma)^2\frac{\mathrm{J}_m(\Omega\gamma)}{\gamma\,\mathrm{J}'_m(\Omega\gamma)}-\mathrm{i}\beta\Omega Z \tag{21}$$

Note that $\mathrm{J}_m(\Omega\gamma)/\Omega\gamma\,\mathrm{J}'_m(\Omega\gamma)$ is a meromorphic function of $\Omega^2\gamma^2$ and therefore of σ^2. So K is a meromorphic function of σ with isolated poles and zeros. The zeros, corresponding with the reduced axial wave numbers in the lined part of the duct, are given by

$$\chi(\sigma)=(1-M\sigma)^2\,\mathrm{J}_m(\Omega\gamma)-\mathrm{i}\beta^3 Z\gamma\,\mathrm{J}'_m(\Omega\gamma)=0 \tag{22}$$

denoted by $\sigma=\tau_{m\nu}$, $\nu=1,2,\ldots$, for the rightrunning modes of the lower complex half plane (see figure 2). The only possible candidate of a rightrunning mode from the upper-half plane (which then has to be an instability) will be denoted (following [1]) by $\sigma=\sigma_{HI}$, where the subscript refers to "hydrodynamic instability" (a possible example is found in the upper right corner of figure 2). The poles, corresponding with the reduced axial wave numbers in the hard part of the duct, are given by

$$\gamma^{1-m}\,\mathrm{J}'_m(\Omega\gamma)=0, \tag{23}$$

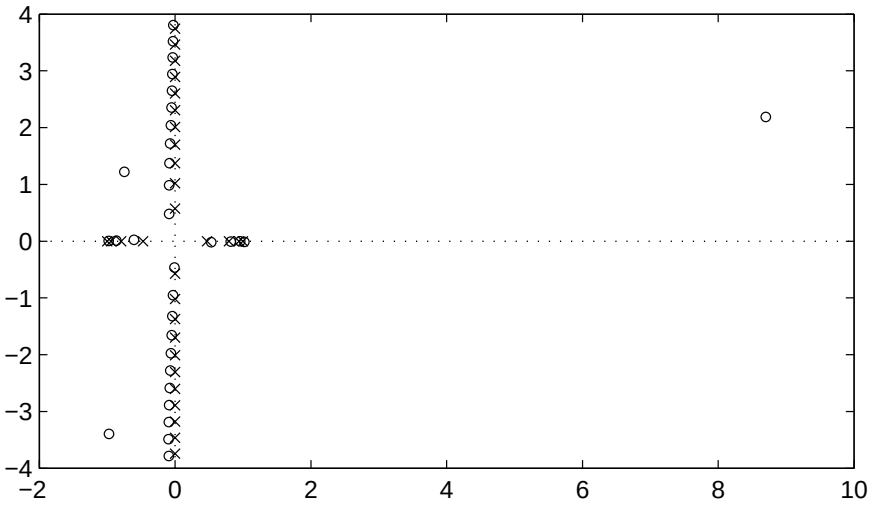

Figure 2. Typical location of soft-wall wave numbers $\tau_{m\nu}$ (indicated by ○) and hard-wall wave numbers $\sigma_{m\nu}$ (indicated by ×). Note the 3 soft-wall surface waves. ($Z = 0.8 - 2\mathrm{i}$, $\omega = 10$, $M = 0.5$, $m = 0$.)

denoted by $\sigma = \sigma_{m\nu}$, implicitly given by $\Omega\gamma = \alpha_{m\nu}$, $\nu = 1, 2, \ldots$ where $\alpha_{m\nu}$ denote the non-trivial zeros of J'_m. For hard-walled ducts, the left and right running reduced wave numbers are symmetric, and so the left-running hard-wall modes are given by $\sigma = -\sigma_{m\nu}$.

In the usual way[29] we split K into functions that are analytic in the upper and in the lower half plane (but note a possible instability pole in the upper half plane that really is to be counted to the lower half plane; see below)

$$K(\sigma) = \frac{K_+(\sigma)}{K_-(\sigma)}. \tag{24}$$

Following appendix A, we introduce the auxiliary split functions N_+ and N_-, satisfying

$$K(\sigma) = \frac{N_+(\sigma)}{N_-(\sigma)} \tag{25}$$

and given by

$$\log N_\pm(\sigma) = \frac{1}{2\pi\mathrm{i}} \int_0^\infty \left[\frac{\ln K(u)}{u - \sigma} - \frac{\ln K(-u)}{u + \sigma} \right] \mathrm{d}u. \tag{26}$$

The $+$ sign corresponds with $\operatorname{Im}\sigma > 0$ or $\operatorname{Im}\sigma = 0$ & $\operatorname{Re}\sigma < 0$, and the $-$ sign with $\operatorname{Im}\sigma < 0$ or $\operatorname{Im}\sigma = 0$ & $\operatorname{Re}\sigma > 0$. (Use for points from the opposite side the definition $K N_- = N_+$.) Following appendix A, we obtain the following asymptotic behaviour

$$N_\pm(\sigma) = \mathcal{O}(\sigma^{\pm 1/2}). \tag{27}$$

When no instability pole crossed the contour, we identify

$$K_+(\sigma) = N_+(\sigma), \quad K_-(\sigma) = N_-(\sigma). \tag{28}$$

When an instability pole σ_{HI} crossed the contour and is to be included among the right-running modes of the lower half-plane, N_- contains the factor $(\sigma - \sigma_{HI})^{-1}$, so the causal split functions are

$$K_+(\sigma) = (\sigma - \sigma_{HI}) N_+(\sigma), \quad K_-(\sigma) = (\sigma - \sigma_{HI}) N_-(\sigma). \tag{29}$$

We continue with our analysis. We substitute the split functions in equation (20) to get

$$K_-(\sigma) P_-(\sigma) + \mathrm{i}\beta\, \mathrm{J}_m(\alpha_{m\mu}) \frac{K_-(\sigma) - K_-(\sigma_{m\mu})}{\Omega(\sigma - \sigma_{m\mu})} = -K_+(\sigma) H_+(\sigma) - \frac{\mathrm{i}\beta\, \mathrm{J}_m(\alpha_{m\mu}) K_-(\sigma_{m\mu})}{\Omega(\sigma - \sigma_{m\mu})} \tag{30}$$

The left hand side is a function analytic in the lower halfplane, while the right hand side is analytic in the upper halfplane. So together they define an entire function E.

From the estimate $h(x) = \mathcal{O}(x^\eta)$ for $x \downarrow 0$ and $\eta > 0$, it follows [29, page 36] that

$$H_+(\sigma) = \mathcal{O}(\sigma^{-\eta-1}) \quad (\sigma \to \infty). \tag{31}$$

This gives us the information to determine E. If there is no instability pole, then $K_+(\sigma)H_+(\sigma) = \mathcal{O}(\sigma^{-\eta-1/2})$, and so E vanishes at infinity and has to vanish everywhere according to Liouville's theorem.[29] If there is an instability pole, we have an extra factor σ and so $K_+(\sigma)H_+(\sigma) = \mathcal{O}(\sigma^{-\eta+1/2})$. This means that if $\eta = 1/2$ (no smooth streamline at $x = 0$, i.e. no Kutta condition), the entire function is only bounded and equal to a constant. If unmodelled physical effects (nonlinearities, viscosity) requires a smooth behaviour of h near $x = 0$, i.e. the Kutta condition, we have to choose $E = 0$, as this yields $\eta = 3/2$. See figure 3.

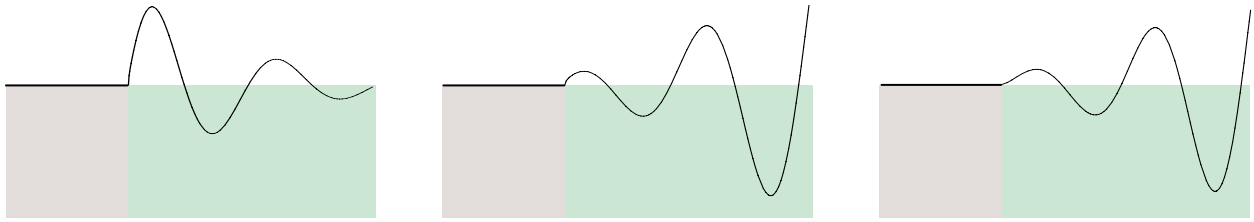

(a) no Kutta condition, no instability (b) no Kutta condition, instability (c) Kutta condition, instability

Figure 3. Types of edge singularity. Note that in the Ingard-Myers model the perturbed wall stream line does *not* cross the wall. It is positioned slightly off the wall at a distance, small compared to a wave length but large compared to any acoustic perturbation.

We will start with the assumption of an instability pole. As we will see, the other case will be automatically included in the formulas, and it will not be necessary to consider both cases separately.

We scale the constant E

$$E = \frac{-\mathrm{i}\beta\,\mathrm{J}_m(\alpha_{m\mu})K_-(\sigma_{m\mu})}{\Omega(\sigma_{HI} - \sigma_{m\mu})}(1-\Gamma) = -\frac{\mathrm{i}\beta}{\Omega}\,\mathrm{J}_m(\alpha_{m\mu})N_-(\sigma_{m\mu})(1-\Gamma) \tag{32}$$

such that $\Gamma = 0$ corresponds with no excitation of the instability (no contribution from σ_{HI}), while $\Gamma = 1$ corresponds with the full Kutta condition. Anything inbetween will correspond to a certain amount of instability wave, but not enough to produce a smooth solution in $x = 0$. It is readily verified that the assumption of *no* instability pole, i.e. $K_+ = N_+$ and $E = 0$, leads to exactly the same formula as with $\Gamma = 0$. So in the following we will identify with condition $\Gamma = 0$ both the situation of no instability pole as well as the situation of an instability that is (for whatever reason) not excited.

The total solution is now given by the following inverse Fourier integral, with a deformation around the pole $\sigma = \sigma_{HI}$ if $\Gamma \neq 0$. (This deformation will result in a residue contribution if $x > 0$.)

$$p = p_{\text{in}} + \frac{\Omega}{2\pi\,\mathrm{i}\beta^2}\,\mathrm{J}_m(\alpha_{m\mu})N_-(\sigma_{m\mu}) \int_{-\infty}^{\infty} \frac{(1-M\sigma)^2\,\mathrm{J}_m(\Omega\gamma r)}{\gamma\,\mathrm{J}'_m(\Omega\gamma)N_+(\sigma)} \left[\frac{1}{\sigma - \sigma_{m\mu}} - \frac{\Gamma}{\sigma - \sigma_{HI}}\right] \exp\Big(\mathrm{i}\frac{\Omega}{\beta}(M-\sigma)x\Big)\,\mathrm{d}\sigma \tag{33}$$

For $x < 0$ we close the contour around the lower complex half-plane, and sum over the residues of the poles in $\sigma = -\sigma_{m\nu}$, the axial wave numbers of the left-running hard-walled modes. We obtain the field

$$p = p_{\text{in}} + \sum_{\nu=1}^{\infty} R_{m\mu\nu}\,\mathrm{J}_m(\alpha_{m\nu}) \exp\Big(\mathrm{i}\frac{\Omega}{\beta}(M + \sigma_{m\nu})x\Big) \tag{34}$$

where

$$R_{m\mu\nu} = \frac{\mathrm{J}_m(\alpha_{m\mu})N_-(\sigma_{m\mu})(1+M\sigma_{m\nu})^2}{\beta^2\sigma_{m\nu}\Big(1 - \dfrac{m^2}{\alpha_{m\nu}^2}\Big)\,\mathrm{J}_m(\alpha_{m\nu})N_+(-\sigma_{m\nu})} \left[\frac{1}{\sigma_{m\nu} + \sigma_{m\mu}} - \frac{\Gamma}{\sigma_{m\nu} + \sigma_{HI}}\right] \tag{35}$$

In particular

$$R_{011} = \frac{1+M}{1-M}\frac{N_-(1)}{N_+(-1)}\left[\frac{1}{2} - \frac{\Gamma}{1+\sigma_{HI}}\right] \tag{36}$$

For the transmitted field in $x > 0$ we close the contour around the upper half-plane and sum over the residues from $\sigma = \tau_{m\nu}, \sigma_{m\mu}$ and (if $\Gamma \neq 0$) $\sigma = \sigma_{HI}$. We note that the residue from $\sigma = \sigma_{m\mu}$ just cancels p_{in}, while the other residues (except from σ_{HI}) are found after rewriting (cf. equation (22))

$$\gamma\, \mathrm{J}'_m(\Omega\gamma) N_+(\sigma) = \frac{\Omega}{\beta^2}\chi(\sigma) N_-(\sigma). \tag{37}$$

We obtain

$$\begin{aligned} p = \sum_{\nu=1}^{\infty} T_{m\mu\nu}\, \mathrm{J}_m(\beta_{m\nu} r) \exp\Big(\mathrm{i}\frac{\Omega}{\beta}(M-\tau_{m\nu})x\Big) \\ - \Gamma\frac{\Omega^2}{\beta^2}\, \mathrm{J}_m(\alpha_{m\mu}) N_-(\sigma_{m\mu}) \frac{(1-M\sigma_{HI})^2}{\beta_{HI}\, \mathrm{J}'_m(\beta_{HI}) N_+(\sigma_{HI})}\, \mathrm{J}_m(\beta_{HI} r) \exp\Big(\mathrm{i}\frac{\Omega}{\beta}(M-\sigma_{HI})x\Big) \end{aligned} \tag{38}$$

where $\beta_{m\nu} = \Omega\gamma(\tau_{m\nu})$, $\beta_{HI} = \Omega\gamma(\sigma_{HI})$, and

$$T_{m\mu\nu} = -\frac{\beta\, \mathrm{J}_m(\alpha_{m\mu}) N_-(\sigma_{m\mu})(1-M\tau_{m\nu})^2}{\chi'(\tau_{m\nu}) N_-(\tau_{m\nu})}\left[\frac{1}{\tau_{m\nu}-\sigma_{m\mu}} - \frac{\Gamma}{\tau_{m\nu}-\sigma_{HI}}\right], \tag{39}$$

while $\chi'(\tau_{m\nu})$ can be further specified to be

$$\chi'(\tau_{m\nu}) = -\mathrm{i}\beta^2 Z\, \mathrm{J}_m(\beta_{m\nu})\left[\omega\tau_{m\nu}\Big(1 - \frac{m^2}{\beta_{m\nu}^2} - \frac{\Lambda_{m\nu}^4}{(\omega\beta_{m\nu}Z)^2}\Big) - \frac{2\mathrm{i}M\Lambda_{m\nu}}{\omega Z}\right], \quad \Lambda_{m\nu} = \frac{\omega(1-M\tau_{m\nu})}{\beta^2}. \tag{40}$$

(This expression may be compared with (16) of [35].)

IV. Causality

To determine the direction of propagation of the modes, and thus detect any possible instability, we have available the following causality criteria:

- The Briggs-Bers[3–5] formalism, where analyticity in the whole lower complex ω-plane is enforced by tracing the poles for fixed $\mathrm{Re}(\omega)$, and $\mathrm{Im}(\omega)$ running from 0 to $-\infty$.
- The Crighton-Leppington[12,26] formalism, where analyticity in the whole lower complex ω-plane is enforced by tracing the poles for fixed $|\omega|$, and $\arg(\omega)$ running from 0 to $-\frac{1}{2}\pi$.

Interestingly, these two methods give conflicting results as to the existence or otherwise of instability waves, and in fact it turns out that it is only the Crighton & Leppington approach which can be applied in this case. However, since the Briggs-Bers method is in common use we will first describe its predictions in some detail, before explaining why it is actually inapplicable here. We will then present the results from the (legitimate) application of the Crighton & Leppington procedure.

For definiteness we will model the complex, frequency-dependent impedance as a simple mass-spring-damper system

$$Z(\omega) = R + \mathrm{i}a\omega - \frac{\mathrm{i}b}{\omega}, \tag{41}$$

which satisfies the fundamental requirements for Z to be physical and passive (see e.g. [36]), viz. Z is analytic and non-zero in $\mathrm{Im}(\omega) < 0$, $Z(\omega) = Z^*(-\omega)$ and $\mathrm{Re}(Z) > 0$. We will briefly consider another possible model at the end of this section.

Turning first to the Briggs-Bers method, sample results are presented on the left of figures 4 & 5. Note that in figure 4 the instability wave starts in the first quadrant of the κ plane, but then crosses the real axis as $\mathrm{Im}(\omega) \to -\infty$. The Briggs-Bers method therefore predicts that this mode propagates downstream (i.e. its group velocity points in the downstream direction) and that it is unstable. In contrast, note that in figure 5 the surface mode remains above the κ

axis as $\mathrm{Im}(\omega) \to -\infty$, so that the Briggs-Bers method predicts that this mode propagates in the upstream direction and decays. It is straightforward to derive a criterion to distinguish between these two different cases, by considering the behaviour of the corresponding root of the dispersion relation (22) as $\mathrm{Im}(\omega) \to -\infty$. We write

$$\sigma = \mathrm{Im}(\omega)\sigma_0 + \sigma_1 + \mathcal{O}(\mathrm{Im}(\omega)^{-1}), \tag{42}$$

and then note that

$$\gamma \frac{\mathrm{J}_m'(\Omega\gamma)}{\mathrm{J}_m(\Omega\gamma)} \sim \mathrm{Im}(\omega)\sigma_0 + \sigma_1 + \mathcal{O}(\mathrm{Im}(\omega)^{-1}). \tag{43}$$

Substituting this result into (22) and equating powers of $\mathrm{Im}(\omega)$, we find an expansion for the surface-wave mode number in the form

$$\kappa = \frac{\mathrm{Im}(\omega)^2 a\beta}{M^2} - \frac{\mathrm{Im}(\omega) R\beta}{M^2} + \mathrm{i}\frac{\mathrm{Im}(\omega)}{\beta^2 M^2}\left[M(2-M^2) - 2a\beta^3\,\mathrm{Re}(\omega)\right] + \ldots. \tag{44}$$

From this expression we can see straightaway that in the Briggs-Bers method instability will be predicted (i.e. the mode approaches infinity through the lower half of the κ plane as $\mathrm{Im}(\omega) \to -\infty$) if and only if $M(2-M^2)/2\beta^3\,\mathrm{Re}(\omega) > a$, and this condition exactly matches the behaviour seen in figures 4 & 5. Note that in figure 5(b) the critical value of a for instability is $a = 0.1451$, compared to the value $a = 0.15$ used in the computation, explaining why the trajectory of the mode is almost parallel to the real κ axis.

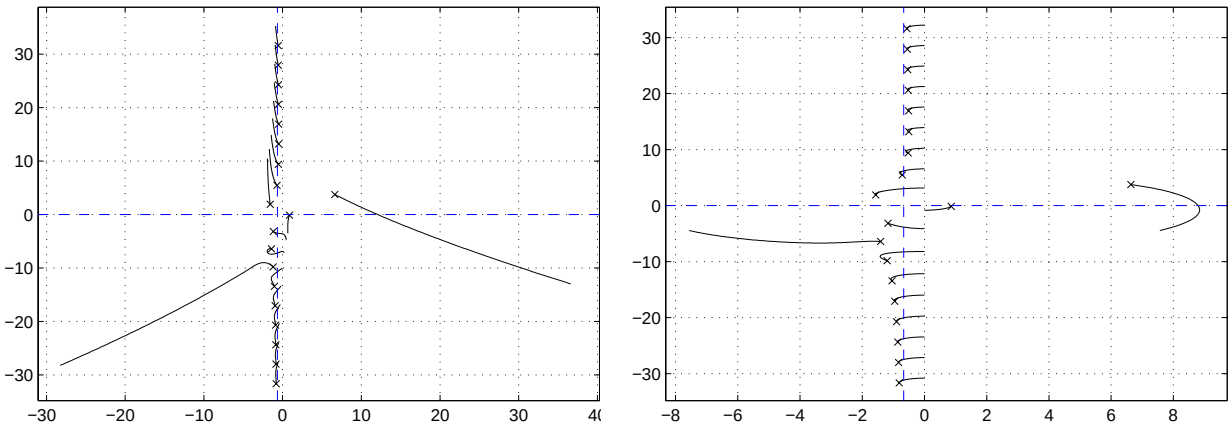

Figure 4. Causality contours for complex ω according to the Briggs-Bers (left) and the Crighton-Leppington (right) formalism. The crosses indicate the location of the modes when $\mathrm{Im}(\omega) = 0$. Both criteria agree in their conclusion about the instability. ($Z = 1 - 0.9\mathrm{i}$, $\omega = 1$, $M = 0.5$, $m = 0$, $a = 0.1$, $b = 1$.)

Unfortunately, the Briggs-Bers predictions described in the previous paragraph cannot be applied to our real problem. This is because there is a rather subtle, but crucial, technical condition which needs to be satisfied before the Briggs-Bers method can be used. What is required is that the system has a finitely-bounded temporal growth rate for all real κ, which allows the temporal inversion contour to be located sufficient low in the complex ω plane so as to lie below all singularities in the ω Fourier transform. To be completely specific, consider the linear system

$$\mathcal{D}\left(\mathrm{i}\frac{\partial}{\partial t}, -\mathrm{i}\frac{\partial}{\partial x}\phi\right) = F(t)\delta(x), \tag{45}$$

where $\mathcal{D}$ is a linear operator and $F(t)$ is the forcing such that $F(t) = 0$ for $t < 0$. Fourier transforming in t and x and inverting, we find the solution

$$\phi(x,t) = \frac{1}{4\pi^2}\int_{\mathcal{C}}\int_{\kappa=-\infty}^{\infty} \frac{\overline{F}(\omega)}{\mathcal{D}(\kappa,\omega)}\,\mathrm{e}^{\mathrm{i}\omega t - \mathrm{i}\kappa x}\,\mathrm{d}\kappa\,\mathrm{d}\omega. \tag{46}$$

In order to have the causal response $\phi = 0$ when $t < 0$ we need to choose the temporal inversion contour $\mathcal{C}$ to lie below the singularities (in ω-domain) of

$$\overline{\phi}(x,\omega) = \frac{1}{2\pi}\overline{F}(\omega)\int_{\kappa=-\infty}^{\infty} \frac{\mathrm{e}^{-\mathrm{i}\kappa x}}{\mathcal{D}(\kappa,\omega)}\mathrm{d}\kappa \tag{47}$$

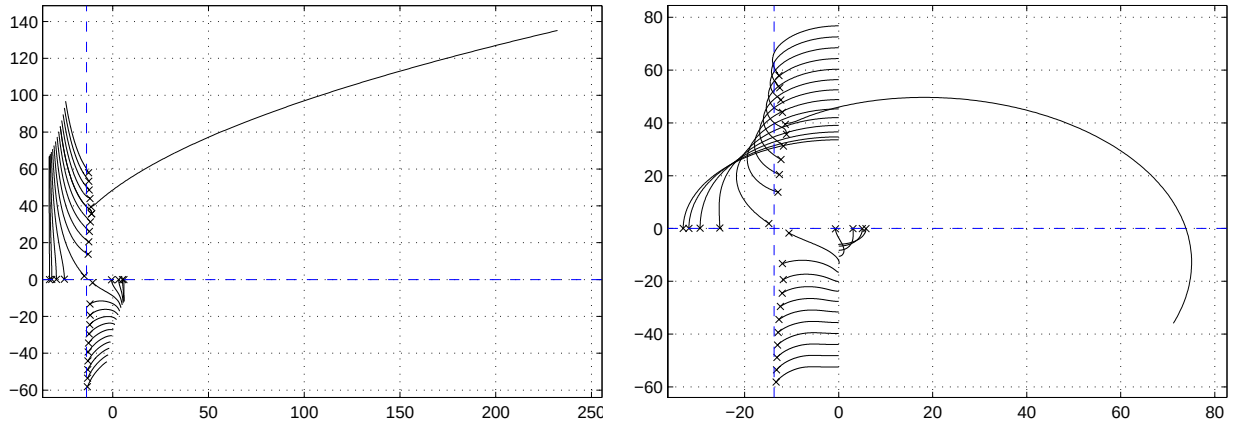

(a) $Z = 1 + 3.335\mathrm{i}$, $\omega = 10$, $M = 0.7$, $m = 0$, $a = 0.335$, $b = 0.15$

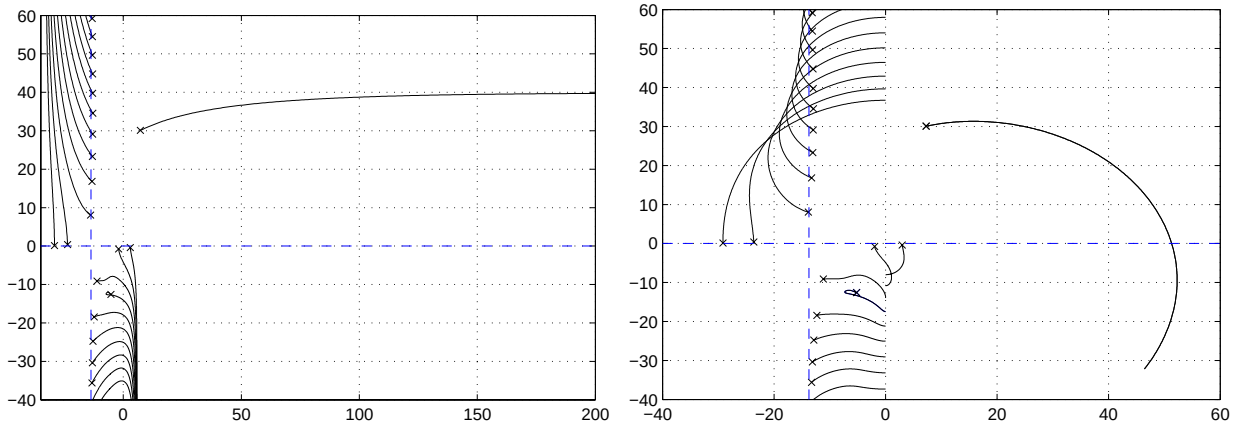

(b) $Z = 1 + 1.385\mathrm{i}$, $\omega = 10$, $M = 0.7$, $m = 5$, $a = 0.15$, $b = 1.15$

Figure 5. Causality contours for complex ω according to the Briggs-Bers (left) and the Crighton-Leppington (right) formalism. The crosses indicate the location of the modes when $\mathrm{Im}(\omega) = 0$. The criteria disagree.

Since $F(t) < 0$ for $t < 0$, it follows that its Fourier transform, $\overline{F}(\omega)$, is analytic in the lower half plane, so that non-analytic behaviour (in ω) of $\overline{\phi}(x, \omega)$ would arise from any singularity of the integrand $\kappa_n(\omega)$, i.e. given by $\mathcal{D}(\kappa, \omega) = 0$, crossing the real κ-axis for some $\omega \in \mathcal{C}$. Hence we need to choose $\mathcal{C}$ such that for any κ_n

$$\mathrm{Im}(\kappa_n(\omega)) \neq 0 \quad \text{for all } \omega \in \mathcal{C}. \tag{48}$$

In particular, if any such κ_n, say $\kappa_i(\omega)$, is found in lower κ-half plane $\{\mathrm{Im}(\kappa) < 0\}$ for $\omega \in \mathcal{C}$ but originates for real ω from $\{\mathrm{Im}(\kappa) > 0\}$, it may have to be interpreted as a right-running instability. In order to confirm this, we need to be able to select $\mathcal{C}$ such that

$$\max_{\omega \in \mathcal{C}} \big[\mathrm{Im}(\kappa_i(\omega))\big] < 0. \tag{49}$$

With this condition fulfilled we find no crossing of the real κ-axis. Formulated in another way, $\mathcal{C}$ can be drawn at a finite depth in the ω plane if the temporal growth rate is bounded for all real κ, i.e. when the inverse expression $\omega_i(\kappa)$ satisfies

$$\min_{\kappa \in \mathbb{R}} \big[\mathrm{Im}(\omega)\big] \equiv -G, \quad \text{where } \; 0 < G < \infty. \tag{50}$$

Returning to our lined-duct dispersion relation (22), we consider large real κ, then it can be shown asymptotically that the unstable surface wave has a growth rate proportional to $\sqrt{\kappa}$, a result which can easily be verified numerically. In

fact, this result is already hinted at in equation (44) above, given the leading-order dependence of κ on the *square* of $\mathrm{Im}(\omega)$. Hence, as $\kappa \to \infty$ the growth rate grows without bound, so that $G = \infty$, the temporal inversion contour $\mathcal{C}$ cannot be drawn below all singularities in the ω plane, and it therefore follows that *the Briggs-Bers method cannot be applied in this case*. This situation mirrors the behaviour in the well-known Kelvin-Helmholtz instability of a vortex sheet, for which $\mathrm{Im}(\omega) \propto \kappa$.

Having decided that the Briggs-Bers method cannot be applied, we now turn to the procedure of Crighton & Leppington.[12,26] The analysis described in [12] concerns the causal solution for scattering of acoustic waves by a semi-infinite vortex sheet, and in many ways can therefore be thought of as being analogous to problem considered in the present paper. Specifically, the difficulty associated with the unbounded growth rate of the vortex sheet is handled in [12,26] by first supposing that the argument of ω is close to (with the present sign convention) $-\frac{1}{2}\pi$. This approach is guaranteed to yield a causal result, since the solution then decays to zero as $t \to -\infty$. Once the Fourier transform has been determined with imaginary ω, the idea is then to attempt to analytically continue the Fourier transform back to the physically-relevant case of real ω. So we set

$$\omega = |\omega| \exp(\mathrm{i}\varphi), \tag{51}$$

and allow φ to increase from $-\frac{1}{2}\pi$ to 0. As φ increases, the singularities in the Fourier transform will move in the κ plane, and to retain analyticity we must deform the κ inversion contour so as to prevent any singularities crossing it. The singularities correspond to the κ roots of (22), and their motion in typical cases is shown in figures 4 and 5. Note that in each case it is only the single surface wave which crosses the real κ axis, having started in the lower half of the κ plane when $\varphi = -\frac{1}{2}\pi$. It therefore follows that, in order to avoid a pole crossing, the κ inversion contour must be deformed so as to run above this pole. This means that the surface wave is picked up when the spatial contour is closed in the lower half plane for $x > 0$, and corresponds to a downstream instability. We can therefore conclude that *in each of the cases described in figures 4 & 5 the Crighton-Leppington method predicts that the system is unstable.*

For the special case of a semi-infinite 2D half-space in the incompressible limit it was shown in [1] analytically that the system is unstable according to the Crighton-Leppington procedure. In general, however, it appears that in order to use this procedure to test the stability of our system we need to solve the dispersion relation numerically, tracking the progress of the possible instability in the κ plane as φ is increased from $-\frac{1}{2}\pi$ to 0. Additional to the incompressible limit, we can make further algebraic progress for large values of $\mathrm{Re}(\omega)$. In much the same way as for the Briggs-Bers method, we write

$$\sigma = |\omega| \exp(\mathrm{i}\varphi)\sigma_0 + \sigma_1 + \mathcal{O}(|\omega|^{-1}), \tag{52}$$

and after some algebra find that the unstable surface wave is given by

$$\kappa = -\frac{\beta a |\omega|^2}{M^2} \exp(2i\varphi) + \left(\frac{i\beta^3 R}{M^2} + \frac{2}{M} - M \right) \frac{|\omega| \exp(\mathrm{i}\varphi)}{\beta^2} + \mathcal{O}(|\omega|^{-1}). \tag{53}$$

We now follow the Crighton-Leppington procedure of increasing φ from $-\frac{1}{2}\pi$ to 0, and we see from (53) that $\mathrm{Im}(\kappa) < 0$ when $\varphi = -\frac{1}{2}\pi$ (since $M < 1$) and $\mathrm{Im}(\kappa) > 0$ when $\varphi = 0$ (since $R > 0$). This shows us that this mode has crossed the real κ axis as φ is increased, so that it is indeed a genuine instability. Note that even if $a = 0$ the mode still crosses the real κ axis, although in this case the typical spatial growth rates are rather smaller, scaling on $|\omega|$ rather than $|\omega^2|$.

In summary, we can conclude that our system is genuinely unstable for the situations described in figures 4 & 5, as well as in the limit of large real frequency. It should be noted, however, that this conclusion may be dependent on the functional dependence of Z on ω, and different impedance models need to be studied on a case-by-case basis. We do note that for another common case, the Helmholtz-resonator model, the conclusion of instability at large $\mathrm{Re}(\omega)$ is also obtained. Writing (for positive constants m and L)

$$Z = R + \mathrm{i}m\omega - \mathrm{i}\cot(\omega L), \tag{54}$$

and noting that $\cot z \to i$ as $z \to \infty$ with $\mathrm{Im}(z) < 0$, we see that the large-$\mathrm{Re}(\omega)$ expansion for the wavenumber is again given by (53), but with R replaced by $R + 1$. It then follows that the mode still crosses the real κ-axis as φ is increased, so that the system is again unstable.

V. Low-frequency asymptotics

An interesting limit in the present context is the one for small ω. In this case only the reflection coefficient R_{011} of the plane wave is of interest. We have for small ω

$$K(\sigma) = -2\frac{(1 - M\sigma)^2}{\beta^2 \gamma(\sigma)^2} + \mathcal{O}(\omega) \quad (\omega \to 0). \tag{55}$$

The double zeros $\sigma = M^{-1}$ arise from two modes, one from the upper half plane and one from the lower half plane, that meet each other at $\omega = 0$. These modes are of surface wave type[1] because the radial wave number is purely imaginary, but for low ω the radial decay is so slow that their confinement to the wall inside the duct is meaningless. The mode from the upper half plane is (in all cases considered) the instability σ_{HI}. The other one is in the nomenclature of [1] the right-running acoustic surface wave σ_{SR}. In the present notation it is a mode from the set $\{\tau_{0\nu}\}$, say[b], τ_{01} or (to avoid any ambiguity) τ_{01}^{+}. For smal but non-zero ω they are asymptotically given by

$$\sigma_{HI} = M^{-1} + \tfrac{1}{2}(1+\mathrm{i})\beta^2 M^{-2}\sqrt{\omega Z} + \ldots \tag{56a}$$

$$\tau_{01}^{+} = M^{-1} - \tfrac{1}{2}(1+\mathrm{i})\beta^2 M^{-2}\sqrt{\omega Z} + \ldots \tag{56b}$$

This is illustrated by figure 6. The first two left and right-running modes are drawn as a function of $Z = 1 + \mathrm{i}\lambda$, where λ is varied from ∞ (hard wall) to $-\infty$ (again hard wall). Starting as the right-running hard-wall plane wave $\sigma_{01} = 1$, τ_{01}^{+} becomes slightly complex, resides near M^{-1} when $\lambda = 0$, but returns to its starting hard-wall value when $\lambda \to -\infty$. The second right-running mode τ_{02}^{+} (the first cut-off) disappears to real $-\infty$. The left-running mode τ_{01}^{-} starts as the hard-wall plane-wave mode $-\sigma_{01} = -1$, then moves to the right, resides near M^{-1} when $\lambda = 0$ (where it apparently has changed its character and has become a *right*-running instability wave !) and then, instead of returning to its original hard-wall value, it disappears to real $+\infty$. Its position has been taken over by the second left-running mode τ_{02}^{-}.

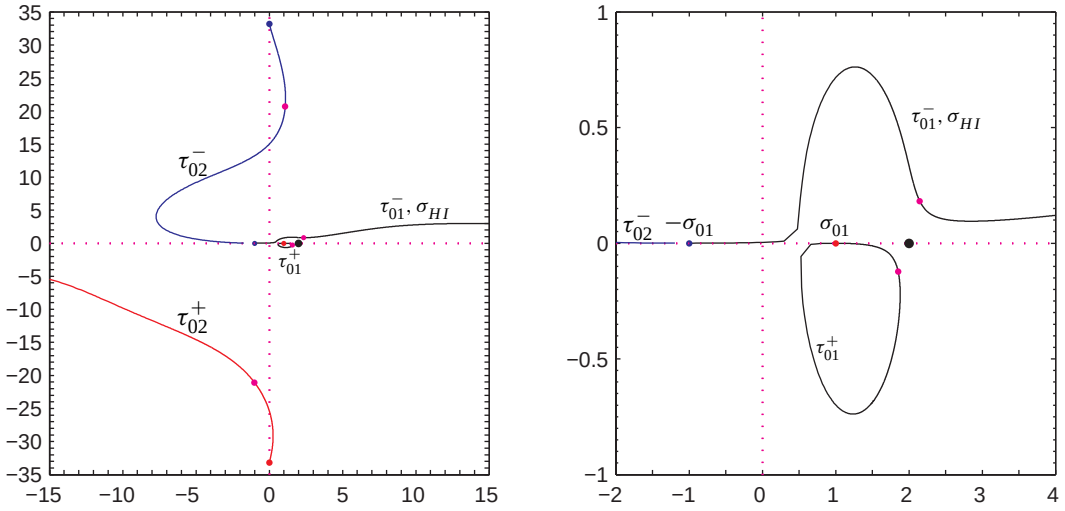

(a) $\omega = 0.1$, $\mathrm{Re}(Z) = 1$, $m = 0$, $M = 0.5$

(b) $\omega = 0.01$, $\mathrm{Re}(Z) = 1$, $m = 0$, $M = 0.5$

Figure 6. Modal wave numbers $\tau_{0\nu}^{\pm}$ as they traverse the complex σ-plane for varying impedance $Z = 1 + \mathrm{i}\lambda$.

Now we can approximate the split functions

$$N_{+}(\sigma) \simeq -2\frac{1 - M\sigma}{\beta^2(1-\sigma)}, \quad N_{-}(\sigma) \simeq \frac{1+\sigma}{1 - M\sigma}, \tag{57}$$

not necessarily with the same multiplicative factor as would arise from representation (A.9). This yields for the plane wave reflection coefficient

$$R_{011} \simeq -\frac{1+M}{1-M}\Big(1 - \frac{2M\Gamma}{1+M}\Big) + \ldots \quad (\omega \to 0), \tag{58}$$

resulting in the remarkably different values $R_{011} = -1$ for $\Gamma = 1$ and $R_{011} = -(1+M)/(1-M)$ for $\Gamma = 0$, irrespective of Z (although the limit $Z \to \infty$, $\omega \to 0$ will be non-uniform). This result is exactly the same as found for the low frequency plane wave reflection coefficients of a semi-infinite duct with jet or uniform mean flow.[14,19–22]

[b] There is no obvious way of sorting soft-wall modes; see figure 6.

The instability wave corresponding to (56a), with axial wave number the Strouhal number ω/M, vanishes in pressure, due to the factor $(1 - M\sigma_{HI})$, but survives in the potential or velocity. The transmission coefficient of the wave corresponding to (56b), with the same axial wave number, appears to be

$$T_{011} \simeq \tfrac{1}{2}\Gamma\Big(\frac{1+M}{1-M}\Big)^{1/2} + \dots \tag{59}$$

VI. Results

In order to illustrate the above results we have evaluated numerically (see Appendix A) the reflection coefficients R_{011} of the plane wave mode $m\mu = 01$ into itself as a function of frequency ω, and reflection coefficient R_{111} of the mode $m\mu = 11$ into itself. The impedance is rather arbitrarily picked as $Z = 1 - 2\mathrm{i}$ and the Mach number $M = 0.5$. Both modulus $|R_{.11}|$ and phase $\phi_{.11}$ are plot but for the lower frequencies the plane wave phase is reformulated to an end correction δ_{011}, i.e. the virtual point beyond $x = 0$, scaled by ω, where the wave seems to reflect with condition $|p|$ is minimal. Since

$$\Big|\mathrm{e}^{-\mathrm{i}\frac{\omega}{1+M}x} + R_{011}\,\mathrm{e}^{\mathrm{i}\frac{\omega}{1-M}x}\Big|^2 = 1 + |R_{011}|^2 + 2|R_{011}|\cos\Big(\tfrac{2\omega}{1-M^2}x + \phi_{011}\Big)$$

is minimal if $\frac{2\omega}{1-M^2}x + \phi_{011} = \pi$, so

$$\delta_{011} = (1-M^2)\frac{\pi - \phi_{011}}{2\omega}. \tag{60}$$

In order to facilitate comparison with the low ω-analysis, the results are both given for a small interval $0 \le \omega \le 1$ and a large interval $0 \le \omega \le 15$. (The endcorrection is given only for the small interval because it loses its meaning for larger frequencies.) The most striking result is probably the confirmation of the analytically found reflection coefficients 1 (Kutta condition; figure 7 left) and $(1+M)/(1-M)$ (no Kutta condition; figure 8 left) for $\omega \to 0$, and in addition that the end correction tends to a finite value (Kutta condition; figure 7 right) and to ∞ (no Kutta condition; figure 8 right). This is also in exact analogy with the jet.[21] Note that this behaviour is not related to $\omega = 0$ being a resonance frequency because R_{111} tends to 1 at its first resonance frequency in both cases (figures 11 and 12).

VII. Conclusions

An explicit Wiener-Hopf solution is derived to describe the scattering of duct modes at a hard-soft wall impedance transition at $x = 0$ in a circular duct with uniform mean flow. A mode, incident from the hard-walled upstream part, is scattered into reflected hard-wall and transmitted soft-wall modes. A plausible edge condition at $x = 0$ requires at least a continuous wall streamline $r = 1 + h(x,t)$, no more singular than $h = \mathcal{O}(x^{1/2})$ for $x \downarrow 0$. By analogy with a trailing edge scattering problem, the possibility of vortex shedding from the hard-soft transition would allow us to apply the Kutta condition and require the edge condition to be no more singular than corresponding to $h = \mathcal{O}(x^{3/2})$ for $x \downarrow 0$.

The physical relevance of this Kutta condition is still an open question. It all depends on the direction of propagation of the soft-wall modes. The Wiener-Hopf analysis shows that no Kutta condition can be applied if none of the apparently up-stream running, decaying, soft-wall modes is in reality a downstream-running instability. However, causality analyses in the complex frequency domain, taking into account the frequency dependence of the impedance, indicate that under certain circumstances one soft-wall mode (per circumferential order) is to be considered as an instability. In this cases we may be able to enforce a Kutta condition and thus excite the instability.

As the growth rate of this presumed instability may be very high, it remains to be seen if this result is an artefact of the linearised model or really representative of reality. There is apparently a need for clarifying and distinguishing experiments to be carried out.

We presented the results for either cases (Kutta and no Kutta condition), and showed that the difference is, for certain choices of parameters, big enough for experimental verification. In particular, the pressure reflection coefficient for the plane wave in the low Helmholtz number regime is near unity for Kutta, and near $(1+M)/(1-M)$ for the no Kutta condition case.

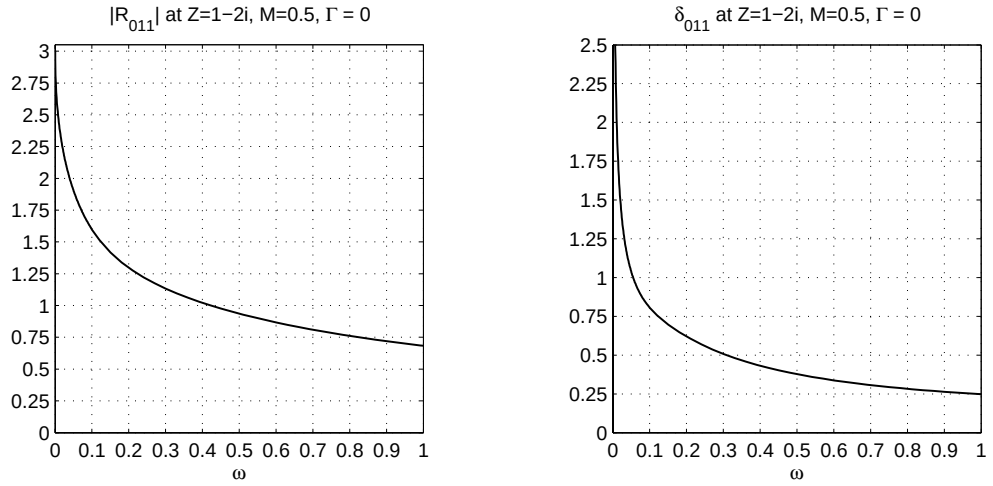

Figure 7. Modulus of reflection coefficient and end correction for plane wave $m\mu = 01$ into 01, where plane wave is incident from hard-walled section to lined section with impedance $Z = 1 - 2\mathrm{i}$, while $M = 0.5$. Without Kutta condition at $x = 0$.

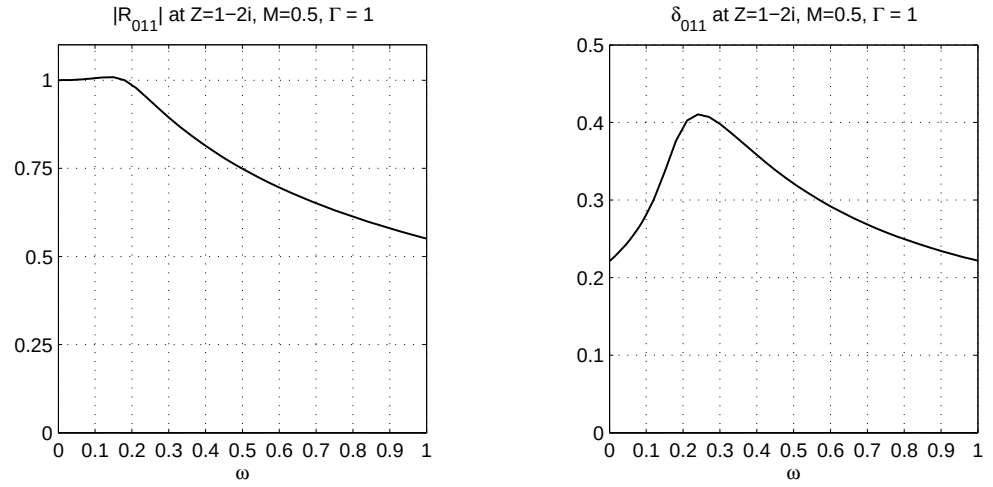

Figure 8. Modulus of reflection coefficient and end correction for plane wave $m\mu = 01$ into 01, where plane wave is incident from hard-walled section to lined section with impedance $Z = 1 - 2\mathrm{i}$, while $M = 0.5$. With Kutta condition at $x = 0$.

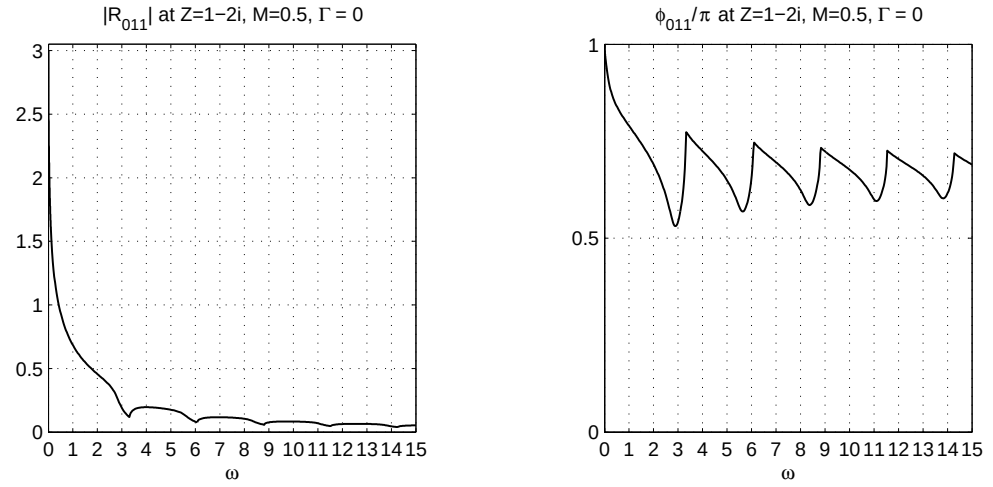

Figure 9. Modulus and phase of reflection coefficient for plane wave $m\mu = 01$ into 01. Same conditions as figure 7 but with larger frequency range.

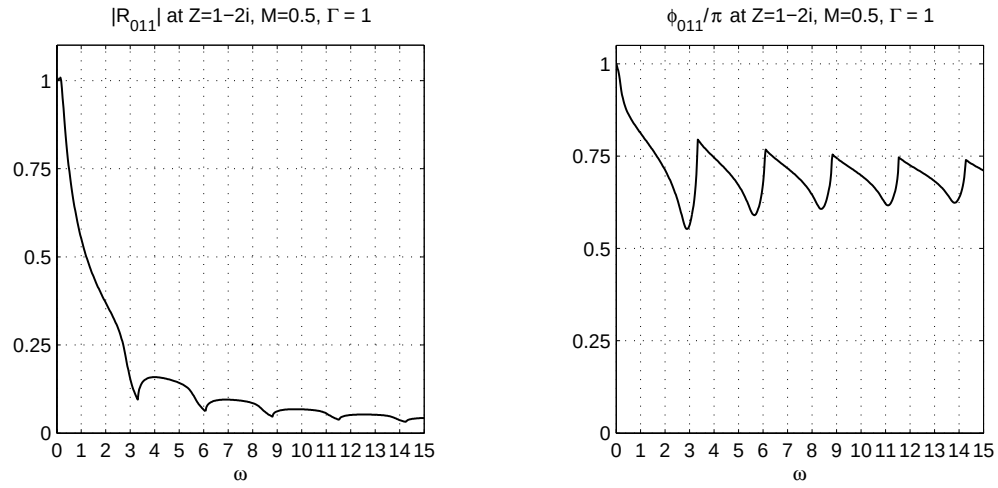

Figure 10. Modulus and phase of reflection coefficient for plane wave $m\mu = 01$ into 01. Same conditions as figure 8 but with larger frequency range.

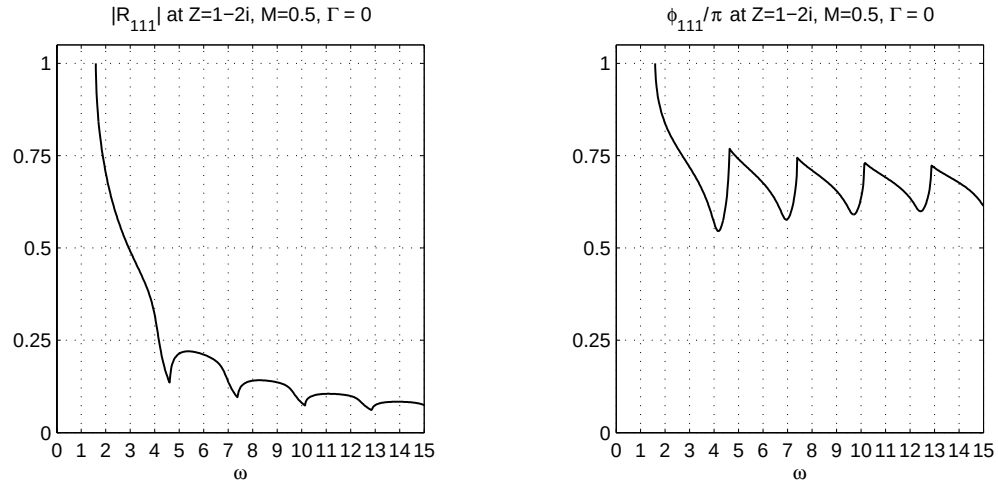

Figure 11. Modulus and phase of reflection coefficient for mode $m\mu = 11$ into 11. Otherwise same conditions as in figure 9.

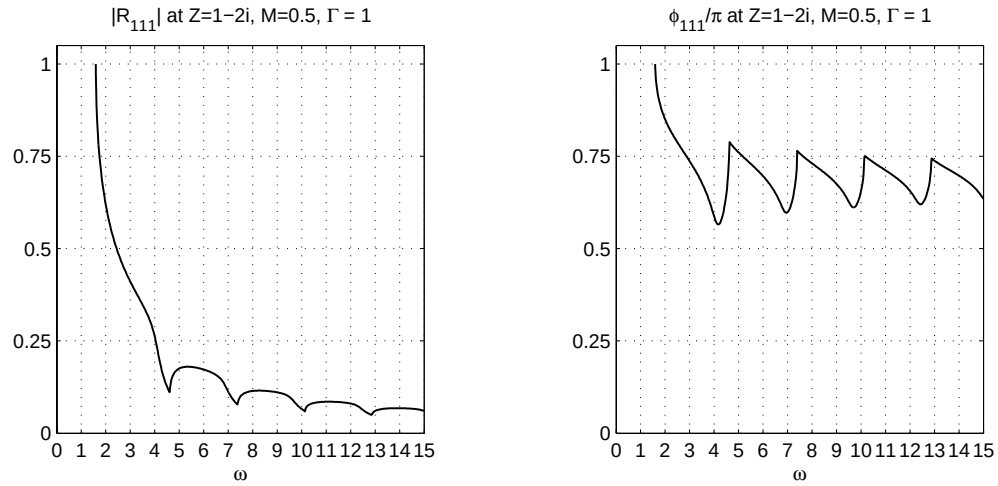

Figure 12. Modulus and phase of reflection coefficient for mode $m\mu = 11$ into 11. Otherwise same conditions as in figure 10.

A. Appendix

Split functions

The complex function $K(\sigma)$ has poles and zeros in the complex plane, in particular also along the real axis. We need to evaluate K, written as a quotient of two function that are analytic in upper and lower halfplane, along the real κ-axis. For reasons of causality we need to start the analysis with a complex-valued ω (with $\mathrm{Im}(\omega) < 0$), see section IV. In that case the zeros and poles and the real κ-axis, mapped (see (13)) into the σ-plane, are typically shifted into the complex plane as indicated in figure 13 (the κ-axis really rotates around $\sigma = M$ instead of 0, but as long as we remain in the region of analyticity we can shift the contour to the right). A set of split functions can now be constructed as follows. We want to write $K(\sigma)$ as the quotient of a function $K_+(\sigma)$, which is analytic and non-zero in the upper half

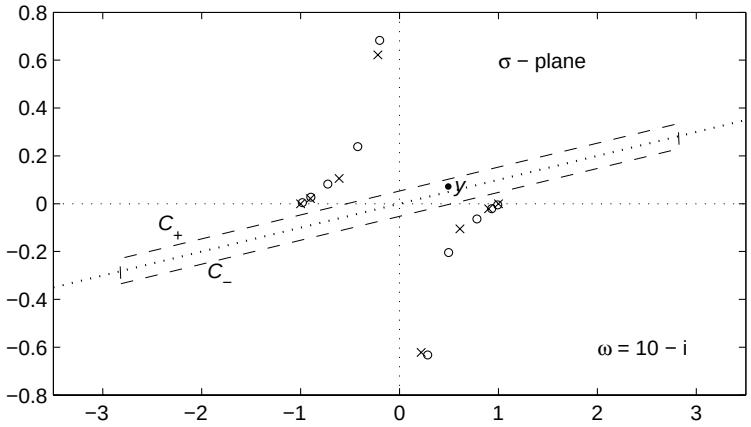

Figure 13. Sketch of zeros and poles of $K(\sigma)$ and contour of integration in the complex σ-plane for complex ω.

plane, and a function $K_-(\sigma)$ which is analytic and non-zero in the lower half plane, while both are at most of algebraic growth at infinity:

$$K(\sigma) = \frac{K_+(\sigma)}{K_-(\sigma)}. \tag{A.1}$$

Construct an elongated rectangle $\mathcal{C} = \mathcal{C}_+ \cup \mathcal{C}_-$ along the rotated κ axis, which makes for $\mathrm{Im}(\omega) < 0$ an angle with the real axis. Select a point y inside $\mathcal{C}$. With $\mathcal{C}$ passing in positive orientation we have

$$\ln K(y) = \frac{1}{2\pi \mathrm{i}} \oint_C \frac{\ln K(u)}{u - y}\, \mathrm{d}u. \tag{A.2}$$

Let the ends of C tend to $\pm\infty$ symmetrically. Since

$$K(\sigma) \sim \frac{\Omega M^2}{\beta^2}\sigma - \frac{2M\Omega}{\beta^2} - \mathrm{i}\beta\Omega Z \;\; (\sigma \to \infty), \quad K(\sigma) \sim -\frac{\Omega M^2}{\beta^2}\sigma + \frac{2M\Omega}{\beta^2} - \mathrm{i}\beta\Omega Z \;\; (\sigma \to -\infty), \tag{A.3}$$

the contributions from the ends cancel each other to leading order, such that the total contribution tends to 0. In particular,

$$\lim_{L\to\infty} \int_{-L}^{L} \frac{\ln K(u)}{u - y}\, \mathrm{d}u = \lim_{L\to\infty} \int_0^L \frac{\ln K(u)}{u - y} - \frac{\ln K(-u)}{u + y}\, \mathrm{d}u = \int_0^\infty \left[\frac{\ln K(u)}{u - y} - \frac{\ln K(-u)}{u + y}\right] \mathrm{d}u \tag{A.4}$$

because

$$\frac{\ln K(u)}{u - y} - \frac{\ln K(-u)}{u + y} = \frac{2y}{u^2} \ln\left(\frac{\Omega M^2}{\beta^2}\right) + \ldots \tag{A.5}$$

converges. Thus we can write

$$\ln K(y) = \frac{1}{2\pi \mathrm{i}} \int_{C_-} \frac{\ln K(u)}{u - y}\, \mathrm{d}u - \frac{1}{2\pi \mathrm{i}} \int_{C_+} \frac{\ln K(u)}{u - y}\, \mathrm{d}u. \tag{A.6}$$

We can identify, respectively, $\ln(K_+)$ and $\ln(K_-)$ with the first and second integral to get

$$K_+(y) = \exp\Big[\frac{1}{2\pi \mathrm{i}} \int_{C_-} \frac{\ln K(u)}{u-y}\,\mathrm{d}u\Big], \quad K_-(y) = \exp\Big[\frac{1}{2\pi \mathrm{i}} \int_{C_+} \frac{\ln K(u)}{u-y}\,\mathrm{d}u\Big], \tag{A.7}$$

because the respective domains can be extended in upward and downward direction without passing any singularities (i.c. the integration contour). If we let $\mathrm{Im}(\omega) \uparrow 0$, we obtain the sought split functions $K_\pm$ for real ω, provided we allow for any possible contour deformation if an instability pole crosses the real axis (see section IV). It is, however, more convenient not to retain this deformed contour but write

$$K(\sigma) = \frac{N_+(\sigma)}{N_-(\sigma)} \tag{A.8}$$

where both N_+ and N_- are now always given by the expression

$$\log N_\pm(\sigma) = \frac{1}{2\pi \mathrm{i}} \int_0^\infty \left[\frac{\ln K(u)}{u-\sigma} - \frac{\ln K(-u)}{u+\sigma}\right] \mathrm{d}u \tag{A.9}$$

with the $+$ sign corresponding with $\mathrm{Im}\,\sigma > 0$ or $\mathrm{Im}\,\sigma = 0$ & $\mathrm{Re}\,\sigma < 0$, and the $-$ sign with $\mathrm{Im}\,\sigma < 0$ or $\mathrm{Im}\,\sigma = 0$ & $\mathrm{Re}\,\sigma > 0$. (Use for points from the opposite side the definition $K N_- = N_+$.) As the split functions are defined up to a multiplicative constant that is determined by the method of calculation, It is instructive to note that constants and simple products are split by (A.9) as follows.

$$c = \frac{c^{1/2}}{c^{-1/2}}, \quad (\sigma - c_+)(\sigma - c_-) = \frac{-\mathrm{i}(\sigma - c_-)}{-\mathrm{i}(\sigma - c_+)^{-1}} \quad (\mathrm{Im}(c_\pm) \gtrless 0). \tag{A.10}$$

When no instability pole crossed the contour, we identify

$$K_+(\sigma) = N_+(\sigma), \quad K_-(\sigma) = N_-(\sigma). \tag{A.11}$$

When an instability pole σ_{HI} crossed the contour, and is to be included among the right-running modes of the lower half-plane, we write

$$K_+(\sigma) = (\sigma - \sigma_{HI}) N_+(\sigma), \quad K_-(\sigma) = (\sigma - \sigma_{HI}) N_-(\sigma). \tag{A.12}$$

When we write

$$K(\sigma) = \mathrm{i}\Omega M^2 \beta^{-2} \gamma(\sigma) L(\sigma), \tag{A.13}$$

then L is a well-behaved function, satisfying $L(\sigma) \to 1$ both for $\sigma \to \infty$ and $-\infty$, and can be split by the present method into functions that remain bounded (see [29], p.15, Theorem C). The factor $\gamma(\sigma)$ can be split by inspection into the quotient of $(1-\sigma)^{1/2}$ and $(1+\sigma)^{-1/2}$. As a result we have the asymptotic estimates

$$N_+(\sigma) = \mathcal{O}(\sigma^{1/2}), \quad N_-(\sigma) = \mathcal{O}(\sigma^{-1/2}) \quad \text{for } \sigma \to \pm\infty, \tag{A.14}$$

leading to corresponding behaviour for K_+ and K_-, depending on the included instability pole.

Numerical evaluation of $K_\pm$

For numerical evaluation of the split functions, we need to evaluate the integral (A.9). First, we have to deal with any possible zeros and poles along the real axis. A natural way to avoid them is by deforming the contour into the upper complex plane, but taking good care to avoid any crossing of other poles or zeros (cf. [22]) A suitable choice was found to be given by the parameterisation $u = \xi(t)$ where

$$\xi(t) = t + \mathrm{i}d\frac{4t/q}{3 + (t/q)^4}, \qquad 0 \le t < \infty. \tag{A.15}$$

$q + \mathrm{i}d$ denotes the position of the top of the indentation (see figure 14). d and q are adjustable constants and have to be chosen such that q is large enough to avoid the real wavenumbers (usually between 0.5 and 1), while d is positive but not too large in order to avoid closing in surface waves. This was tested in all cases considered by visual inspection. For example for very small Z (see [1]), and for $m = 0$ and very small ω, there is a surface wave that approaches the real value $\sigma = M^{-1}$ from above. The next step is to change the infinite integral into a finite integral by the transformation

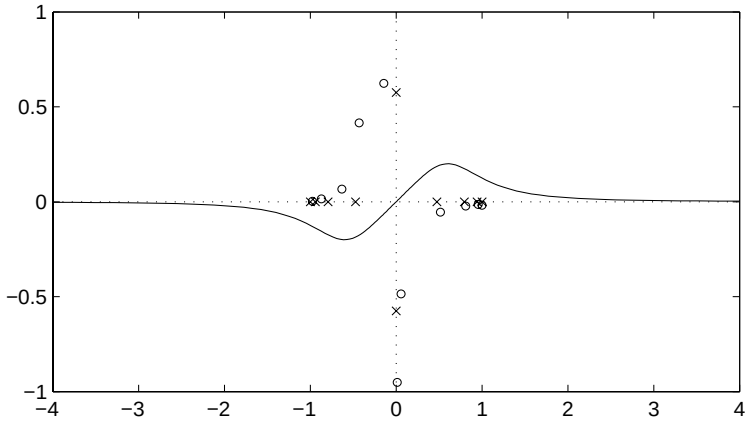

Figure 14. Deformed integration contour given by equation (A.15). Both $u = \xi(t)$ and $u = -\xi(t)$ are drawn. ($Z = 2 - \mathrm{i}$, $\omega = 10$, $M = 0.5$, $m = 0$, $d = 0.2$, $q = 0.6$.)

$t = \zeta(s)$ where

$$\zeta(s) = \frac{s}{(1-s)^2}, \qquad 0 \le s \le 1. \tag{A.16}$$

This particular choice ensures that the resulting integral is easily evaluated by standard routines because the limiting value of the integrand at $s = 1$ is just zero. This is seen as follows. After both transformations we have

$$\int_0^\infty \left[\frac{\ln K(u)}{u-\sigma} - \frac{\ln K(-u)}{u+\sigma}\right] \mathrm{d}u = \int_0^1 \left[\frac{\ln K(\xi(\zeta(s)))}{\xi(\zeta(s))-\sigma} - \frac{\ln K(-\xi(\zeta(s)))}{\xi(\zeta(s))+\sigma}\right] \xi'(\zeta(s))\zeta'(s)\,\mathrm{d}s \tag{A.17}$$

For $s \uparrow 1$, i.e. $u \to \infty$, we have

$$\left[\frac{\ln K(\xi(\zeta(s)))}{\xi(\zeta(s))-\sigma} - \frac{\ln K(-\xi(\zeta(s)))}{\xi(\zeta(s))+\sigma}\right] \xi'(\zeta(s))\zeta'(s) = 4\sigma \ln\left(\frac{\Omega M^2}{\beta^2}\right)(1-s) + \cdots \to 0. \tag{A.18}$$

Acknowledgements

S.W. Rienstra's contribution was for the greater part carried out under a grant of the Royal Society at the University of Cambridge. The financial support is greatly acknowledged.

The assistance of Peter in't Panhuis with the implementation of (A.15) and (A.17) is much appreciated.

References

[1]S.W. Rienstra, "A Classification of Duct Modes Based on Surface Waves", *Wave Motion*, 37 (2), 119–135, 2003.

[2]B.J. Tester, "The Propagation and Attenuation of Sound in Ducts Containing Uniform or 'Plug' Flow." *Journal of Sound and Vibration*, 28(2), 151–203, 1973

[3]A. Bers and R.J. Briggs, MIT Research Laboratory of Electronics Report No. 71 (unpublished), 1963

[4]R.J. Briggs, *Electron-Stream Interaction with Plasmas*, Monograph no. 29, MIT Press, Cambridge Massachusetts, 1964

[5]A. Bers, "Space-Time Evolution of Plasma Instabilities – Absolute and Convective", *Handbook of Plasma Physics: Volume 1 Basic Plasma Physics*, edited by A.A. Galeev and R.N. Sudan, North Holland Publishing Company, Chapter 3.2, 451 – 517, 1983

[6]W. Koch, W. Möhring, "Eigensolutions for liners in uniform mean flow ducts", *AIAA Journal*, 21, 200–213, 1983.

[7]P.G. Daniels, "On the Unsteady Kutta Condition", *Quarterly Journal of Mechanics and Applied Mathematics*, 31, 49–75, 1985

[8]S.W. Rienstra, "Sound Diffraction At A Trailing Edge", *Journal of Fluid Mechanics*, 108, 443–460, 1981.

[9]M.E. Goldstein, "The coupling between flow instabilities and incident disturbances at a leading edge, *Journal of Fluid Mechanics*, 104, 217–246, 1981

[10]D.G. Crighton and D. Innes, "Analytical models for shear-layer feed-back cycles, AIAA81-0061, AIAA Aerospace Sciences Meeting, 19th, St. Louis, Mo., Jan. 12-15, 1981

[11]J.E. Ffowcs Williams, *Annual Review of Fluid Mechanics*, 9, 447-468, 1977.

[12]D.G. Crighton and F.G. Leppington, "Radiation Properties of the Semi-Infinite Vortex Sheet: the Initial-Value Problem", *Journal of Fluid Mechanics* 64(2), 393–414, 1974

[13]R.M. Munt, " The interaction of sound with a subsonic jet issuing from a semi-infinite cylindrical pipe", *Journal of Fluid Mechanics*, 83(4), 609–640, 1977

[14]R.M. Munt, " Acoustic radiation properties of a jet pipe with subsonic jet flow: I. The cold jet reflection coefficient", Journal of Sound and Vibration, 142(3), 413–436, 1990

[15]J.D. Morgan, "The interaction of sound with a semi-infinite vortex sheet", *Quarterly Journal of Mechanics and Applied Mathematics*, 27, 465–487, 1974

[16]D.W. Bechert, "Sound absorption caused by vorticity shedding, demonstrated with a jet flow", *Journal of Sound and Vibration*, 70, 389–405, 1980

[17]D.W. Bechert, "Excitation of instability waves in free shear layers. Part 1. Theory", *Journal of Fluid Mechanics*, 186, 47–62, 1988

[18]M.S. Howe, "Attenuation of sound in a low Mach number nozzle flow, *Journal of Fluid Mechanics*, 91, 209–229, 1979

[19]A.M. Cargill, "Low-frequency sound radiation and generation due to the interaction of unsteady flow with a jet pipe", *Journal of Fluid Mechanics*, 121, 59–105, 1982

[20]A.M. Cargill, "Low frequency acoustic radiation from a jet pipe - A second order theory", *Journal of Sound and Vibration*, 83, 339–354, 1982

[21]S.W. Rienstra, "A small Strouhal number analysis for acoustic wave-jet flow-pipe interaction", *Journal of Sound and Vibration*, 86, 539–556, 1983

[22]S.W. Rienstra, "Acoustic Radiation from a Semi-infinite Annular Duct in a Uniform Subsonic Mean Flow", *Journal of Sound and Vibration*, 94(2), 267–288, 1984.

[23]D.G. Crighton, "The Kutta condition in unsteady flow", *Annual Review of Fluid Mechanics*, 17, 411–445, 1985

[24]M.C.A.M. Peters, A. Hirschberg, A.J. Reijnen, and A.P.J. Wijnands, "Damping and reflection coefficient measurements for an open pipe at low Mach and low Helmholtz numbers", *Journal of Fluid Mechanics*, 256, 499–534, 1993

[25]A. Cummings, "Acoustic nonlinearities and power losses at orifices, *AIAA Journal*, 22, 786–792, 1983

[26]D.S. Jones and J.D. Morgan, "The Instability of a Vortex Sheet on a Subsonic Stream under Acoustic Radiation", *Proc. Camb. Phil. Soc.* 72, 465–488, 1972

[27]M.C. Quinn and M.S. Howe, "On the production and absorption of sound by lossless liners in the presence of mean flow", *Journal of Sound and Vibration* 97 (1), 1–9, 1984

[28]S.W. Rienstra, "Hydrodynamic Instabilities and Surface Waves in a Flow over an Impedance Wall", *Proceedings IUTAM Symposium 'Aero- and Hydro-Acoustics' 1985 Lyon*, 483–490, Springer-Verlag, Heidelberg, (ed. G. Comte-Bellot and J.E. Ffowcs Williams), 1986

[29]B. Noble, *Methods based on the Wiener-Hopf Technique*, Pergamon Press, London, 1958.

[30]A.E. Heins and H. Feshbach, "The coupling of two acoustical ducts", *Journal of Mathematics and Physics*, 26, 143–155, 1947.

[31]H. Levine and J. Schwinger, "On the radiation of sound from an unflanged circular pipe", *Journal Phys. Rev.*, 73, 383–406, 1948

[32]K.U. Ingard,"Influence of Fluid Motion Past a Plane Boundary on Sound Reflection, Absorption, and Transmission". *Journal of the Acoustical Society of America* 31(7), 1035–1036, 1959

[33]M.K. Myers, "On the acoustic boundary condition in the presence of flow", *Journal of Sound and Vibration*, 71 (3), 429–434, 1980

[34]M. Abramowitz and I.A. Stegun, *Handbook of Mathematical Functions*, National Bureau of Standards, Dover Publications, Inc., New York, 1964.

[35]S.W. Rienstra and B.J. Tester, "An Analytic Green's Function for a Lined Circular Duct Containing Uniform Mean Flow", AIAA paper 2005-3020, 11th AIAA/CEAS Aeroacoustics Conference, 10-12 May 2005, Monterey, CA, USA

[36]S.W. Rienstra, "1D Reflection at an Impedance Wall", *Journal of Sound and Vibration*, 125, 43–51, 1988.